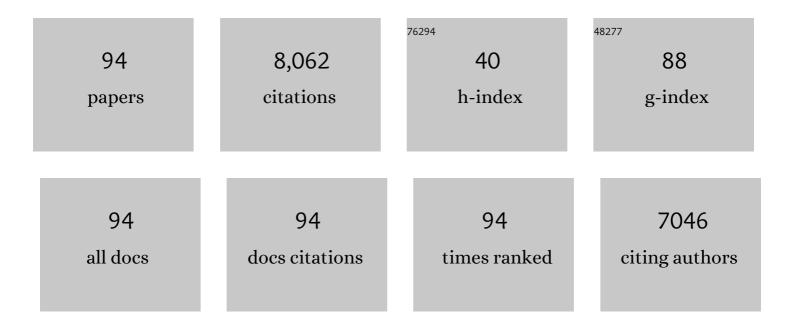
Aleksander Kostka

List of Publications by Year in descending order

Source: https://exaly.com/author-pdf/6370429/publications.pdf Version: 2024-02-01



#	Article	IF	CITATIONS
1	Quantitative analysis of grain boundary diffusion, segregation and precipitation at a sub-nanometer scale. Acta Materialia, 2022, 225, 117522.	3.8	18
2	Influence of Mo/Cr ratio on the lamellar microstructure and mechanical properties of as-cast Al0.75CoCrFeNi compositionally complex alloys. Journal of Alloys and Compounds, 2022, 899, 163183.	2.8	5
3	Effect of off-stoichiometric compositions on microstructures and phase transformation behavior in Ni-Cu-Pd-Ti-Zr-Hf high entropy shape memory alloys. Journal of Alloys and Compounds, 2021, 857, 157467.	2.8	13
4	Influence of low Bi contents on phase transformation properties of VO ₂ studied in a VO ₂ :Bi thin film library. RSC Advances, 2021, 11, 7231-7237.	1.7	5
5	Laser metal deposition of refractory high-entropy alloys for high-throughput synthesis and structure-property characterization. International Journal of Extreme Manufacturing, 2021, 3, 015201.	6.3	27
6	Crystallographic Orientation Analysis of Nanocrystalline Tungsten Thin Film Using TEM Precession Electron Diffraction and SEM Transmission Kikuchi Diffraction. Microscopy and Microanalysis, 2021, 27, 237-249.	0.2	7
7	Laser metal deposition of Al0.6CoCrFeNi with Ti & C additions using elemental powder blends. Surface and Coatings Technology, 2021, 418, 127233.	2.2	6
8	Direct liquid injection chemical vapor deposition of ZrO2 films from a heteroleptic Zr precursor: interplay between film characteristics and corrosion protection of stainless steel. Journal of Materials Research and Technology, 2021, 13, 1599-1614.	2.6	16
9	TEM replica analysis of particle phases in a tempered martensite ferritic Cr steel after long term creep. Materials Characterization, 2021, 181, 111396.	1.9	4
10	Sensing and electrocatalytic activity of tungsten disulphide thin films fabricated <i>via</i> metal–organic chemical vapour deposition. Journal of Materials Chemistry C, 2021, 9, 10254-10265.	2.7	8
11	Spinodal decomposition versus classical γ′ nucleation in a nickel-base superalloy powder: An in-situ neutron diffraction and atomic-scale analysis. Acta Materialia, 2020, 200, 959-970.	3.8	25
12	Phase decomposition in a nanocrystalline CrCoNi alloy. Scripta Materialia, 2020, 188, 259-263.	2.6	9
13	A new metalorganic chemical vapor deposition process for MoS ₂ with a 1,4-diazabutadienyl stabilized molybdenum precursor and elemental sulfur. Dalton Transactions, 2020, 49, 13462-13474.	1.6	12
14	Structure Zone Investigation of Multiple Principle Element Alloy Thin Films as Optimization for Nanoindentation Measurements. Materials, 2020, 13, 2113.	1.3	5
15	High-throughput characterization of Ag–V–O nanostructured thin-film materials libraries for photoelectrochemical solar water splitting. International Journal of Hydrogen Energy, 2020, 45, 12037-12047.	3.8	10
16	Correlation of Microstructure and Properties of Cold Gas Sprayed INCONEL 718 Coatings. Journal of Thermal Spray Technology, 2020, 29, 1455-1465.	1.6	17
17	Effect of Grain Statistics on Micromechanical Modeling: The Example of Additively Manufactured Materials Examined by Electron Backscatter Diffraction. Advanced Engineering Materials, 2020, 22, 1901416.	1.6	5
18	Correlative chemical and structural investigations of accelerated phase evolution in a nanocrystalline high entropy alloy. Scripta Materialia, 2020, 183, 122-126.	2.6	14

#	Article	IF	CITATIONS
19	PEALD of HfO ₂ Thin Films: Precursor Tuning and a New Near-Ambient-Pressure XPS Approach to in Situ Examination of Thin-Film Surfaces Exposed to Reactive Gases. ACS Applied Materials & Interfaces, 2019, 11, 28407-28422.	4.0	21
20	Stress-induced formation of TCP phases during high temperature low cycle fatigue loading of the single-crystal Ni-base superalloy ERBO/1. Acta Materialia, 2019, 168, 343-352.	3.8	39
21	Data regarding the influence of Al, Ti, and C additions to as-cast Al0.6CoCrFeNi compositionally complex alloys on microstructures and mechanical properties. Data in Brief, 2019, 27, 104742.	0.5	1
22	Influence of composition and precipitation evolution on damage at grain boundaries in a crept polycrystalline Ni-based superalloy. Acta Materialia, 2019, 166, 158-167.	3.8	61
23	Columnar to equiaxed transition and grain refinement of cast CrCoNi medium-entropy alloy by microalloying with titanium and carbon. Journal of Alloys and Compounds, 2019, 775, 1068-1076.	2.8	71
24	Validation of a Terminally Amino Functionalized Tetraâ€Alkyl Sn(IV) Precursor in Metal–Organic Chemical Vapor Deposition of SnO 2 Thin Films: Study of Film Growth Characteristics, Optical, and Electrical Properties. Advanced Materials Interfaces, 2019, 6, 1801540.	1.9	9
25	Understanding precipitate evolution during friction stir welding of Al-Zn-Mg-Cu alloy through in-situ measurement coupled with simulation. Acta Materialia, 2018, 148, 163-172.	3.8	64
26	Accelerated atomic-scale exploration of phase evolution in compositionally complex materials. Materials Horizons, 2018, 5, 86-92.	6.4	72
27	Microstructure and mechanical properties in the thin film system Cu-Zr. Thin Solid Films, 2018, 645, 193-202.	0.8	10
28	On the nucleation of planar faults during low temperature and high stress creep of single crystal Ni-base superalloys. Acta Materialia, 2018, 144, 642-655.	3.8	39
29	Segregation Phenomena in Size-Selected Bimetallic CuNi Nanoparticle Catalysts. Journal of Physical Chemistry B, 2018, 122, 919-926.	1.2	18
30	Microstructure and mechanical properties of Al0.7CoCrFeNi high-entropy-alloy prepared by directional solidification. Intermetallics, 2018, 93, 93-100.	1.8	60
31	Indentation size effects in spherical nanoindentation analyzed by experiment and non-local crystal plasticity. Materialia, 2018, 3, 21-30.	1.3	19
32	Phase stability and kinetics of σ-phase precipitation in CrMnFeCoNi high-entropy alloys. Acta Materialia, 2018, 161, 338-351.	3.8	209
33	How evolving multiaxial stress states affect the kinetics of rafting during creep of single crystal Ni-base superalloys. Acta Materialia, 2018, 158, 381-392.	3.8	32
34	Atomic-scale investigation of fast oxidation kinetics of nanocrystalline CrMnFeCoNi thin films. Journal of Alloys and Compounds, 2018, 766, 1080-1085.	2.8	39
35	Kinetics and crystallization path of a Fe-based metallic glass alloy. Acta Materialia, 2017, 127, 341-350.	3.8	47
36	Reasons for the superior mechanical properties of medium-entropy CrCoNi compared to high-entropy CrMnFeCoNi. Acta Materialia, 2017, 128, 292-303.	3.8	803

Aleksander Kostka

#	Article	IF	CITATIONS
37	Microstructure evolution in refill friction stir spot weld of a dissimilar Al–Mg alloy to Zn-coated steel. Science and Technology of Welding and Joining, 2017, 22, 658-665.	1.5	37
38	Short Communication on "Coarsening of Y-rich oxide particles in 9%Cr-ODS Eurofer steel annealed at 1350Ã, Ã,°C― Journal of Nuclear Materials, 2017, 484, 283-287.	1.3	13
39	Transmission Electron Microscopy of a CMSX-4 Ni-Base Superalloy Produced by Selective Electron Beam Melting. Metals, 2016, 6, 258.	1.0	20
40	Palladium Nanoparticles Supported on Nitrogenâ€Doped Carbon Nanotubes as a Releaseâ€andâ€Catch Catalytic System in Aerobic Liquidâ€Phase Ethanol Oxidation. ChemCatChem, 2016, 8, 1269-1273.	1.8	14
41	Double minimum creep of single crystal Ni-base superalloys. Acta Materialia, 2016, 112, 242-260.	3.8	74
42	Tempering behavior of a low nitrogen boron-added 9%Cr steel. Materials Science & Engineering A: Structural Materials: Properties, Microstructure and Processing, 2016, 662, 443-455.	2.6	62
43	Microstructure evolution and critical stress for twinning in the CrMnFeCoNi high-entropy alloy. Acta Materialia, 2016, 118, 152-163.	3.8	823
44	On Local Phase Equilibria and the Appearance of Nanoparticles in the Microstructure of Singleâ€Crystal Niâ€Base Superalloys. Advanced Engineering Materials, 2016, 18, 1556-1567.	1.6	39
45	Deformationâ€Induced Martensite: A New Paradigm for Exceptional Steels. Advanced Materials, 2016, 28, 7753-7757.	11.1	61
46	The crystallographic template effect assisting the formation of stable α-Al2O3 during low temperature oxidation of Fe–Al alloys. Corrosion Science, 2016, 105, 100-108.	3.0	34
47	CNT-TiO2â^'δ Composites for Improved Co-Catalyst Dispersion and Stabilized Photocatalytic Hydrogen Production. Catalysts, 2015, 5, 270-285.	1.6	18
48	Microstructure refinement for high modulus in-situ metal matrix composite steels via controlled solidification of the system Fe–TiB2. Acta Materialia, 2015, 96, 47-56.	3.8	68
49	Advanced Scale Bridging Microstructure Analysis of Single Crystal Niâ€Base Superalloys. Advanced Engineering Materials, 2015, 17, 216-230.	1.6	117
50	Stability of Dealloyed Porous Pt/Ni Nanoparticles. ACS Catalysis, 2015, 5, 5000-5007.	5.5	110
51	Ledges and grooves at γ/γ′ interfaces of single crystal superalloys. Acta Materialia, 2015, 90, 105-117.	3.8	49
52	Nanoindentation studies of the mechanical properties of the μ phase in a creep deformed Re containing nickel-based superalloy. Materials Science & Engineering A: Structural Materials: Properties, Microstructure and Processing, 2015, 634, 202-208.	2.6	72
53	Design of a twinning-induced plasticity high entropy alloy. Acta Materialia, 2015, 94, 124-133.	3.8	618
54	The nucleation of Mo-rich Laves phase particles adjacent to M23C6 micrograin boundary carbides in 12% Cr tempered martensite ferritic steels. Acta Materialia, 2015, 90, 94-104.	3.8	140

#	Article	IF	CITATIONS
55	Mechanisms of subgrain coarsening and its effect on the mechanical properties of carbon-supersaturated nanocrystalline hypereutectoid steel. Acta Materialia, 2015, 84, 110-123.	3.8	60
56	Interface engineering and characterization at the atomic-scale of pure and mixed ion layer gas reaction buffer layers in chalcopyrite thin-film solar cells. Progress in Photovoltaics: Research and Applications, 2015, 23, 705-716.	4.4	20
57	Crystallization, phase evolution and corrosion of Fe-based metallic glasses: An atomic-scale structural and chemical characterization study. Acta Materialia, 2014, 71, 20-30.	3.8	62
58	Interaction of Cobalt Nanoparticles with Oxygen- and Nitrogen-Functionalized Carbon Nanotubes and Impact on Nitrobenzene Hydrogenation Catalysis. ACS Catalysis, 2014, 4, 1478-1486.	5.5	108
59	Sequential Growth of Zinc Oxide Nanorod Arrays at Room Temperature via a Corrosion Process: Application in Visible Light Photocatalysis. ACS Applied Materials & Interfaces, 2014, 6, 18728-18734.	4.0	24
60	On the nucleation of Laves phase particles during high-temperature exposure and creep of tempered martensite ferritic steels. Acta Materialia, 2014, 81, 230-240.	3.8	129
61	Segregation Stabilizes Nanocrystalline Bulk Steel with Near Theoretical Strength. Physical Review Letters, 2014, 113, 106104.	2.9	224
62	Smaller is less stable: Size effects on twinning vs. transformation of reverted austenite in TRIP-maraging steels. Acta Materialia, 2014, 79, 268-281.	3.8	225
63	Enhanced Quantum Confined Stark Effect in a mesoporous hybrid multifunctional system. Solid State Communications, 2014, 187, 48-52.	0.9	2
64	Long-term microstructural stability of oxide-dispersion strengthened Eurofer steel annealed at 800A°C. Journal of Nuclear Materials, 2014, 448, 33-42.	1.3	30
65	Purified oxygen- and nitrogen-modified multi-walled carbon nanotubes as metal-free catalysts for selective olefin hydrogenation. Journal of Energy Chemistry, 2013, 22, 312-320.	7.1	24
66	Simple synthesis of superparamagnetic magnetite nanoparticles as highly efficient contrast agent. Materials Letters, 2013, 95, 186-189.	1.3	35
67	The structural and electronic promoting effect of nitrogen-doped carbon nanotubes on supported Pd nanoparticles for selective olefin hydrogenation. Catalysis Science and Technology, 2013, 3, 1964.	2.1	79
68	Control of Phase Coexistence in Calcium Tantalate Composite Photocatalysts for Highly Efficient Hydrogen Production. Chemistry of Materials, 2013, 25, 4739-4745.	3.2	41
69	Dislocation engineering and its effect on the oxidation behaviour. Materials at High Temperatures, 2012, 29, 116-122.	0.5	4
70	Degradation Mechanisms of Pt/C Fuel Cell Catalysts under Simulated Start–Stop Conditions. ACS Catalysis, 2012, 2, 832-843.	5.5	470
71	Stability investigations of electrocatalysts on the nanoscale. Energy and Environmental Science, 2012, 5, 9319.	15.6	230
72	Direct monophasic replacement of fatty acid by DMSA on SPION surface. Applied Surface Science, 2012, 258, 9685-9691.	3.1	18

#	Article	IF	CITATIONS
73	Friction-stir dissimilar welding of aluminium alloy to high strength steels: Mechanical properties and their relation to microstructure. Materials Science & Engineering A: Structural Materials: Properties, Microstructure and Processing, 2012, 556, 175-183.	2.6	161
74	On the Correlation Between Thermal Cycle and Formation of Intermetallic Phases at the Interface of Laserâ€Welded Aluminumâ€6teel Overlap Joints. Advanced Engineering Materials, 2012, 14, 464-472.	1.6	27
75	Microstructural evolution of a Ni-based superalloy (617B) at 700°C studied by electron microscopy and atom probe tomography. Acta Materialia, 2012, 60, 1731-1740.	3.8	212
76	Synthesis of titanium carbonitride coating layers with star-shaped crystallite morphology. Materials Letters, 2012, 68, 71-74.	1.3	13
77	Size and size distribution of apatite crystals in sauropod fossil bones. Palaeogeography, Palaeoclimatology, Palaeoecology, 2011, 310, 108-116.	1.0	22
78	Effect of Shot-peening on the Oxidation Behaviour of Boiler Steels. Oxidation of Metals, 2011, 76, 233-245.	1.0	41
79	Influence of intermetallic phases and Kirkendall-porosity on the mechanical properties of joints between steel and aluminium alloys. Materials Science & Engineering A: Structural Materials: Properties, Microstructure and Processing, 2011, 528, 4630-4642.	2.6	209
80	Thermal stability of TiAlN/CrN multilayer coatings studied by atom probe tomography. Ultramicroscopy, 2011, 111, 518-523.	0.8	29
81	On the formation and growth of intermetallic phases during interdiffusion between low-carbon steel and aluminum alloys. Acta Materialia, 2011, 59, 1586-1600.	3.8	397
82	Hierarchical microstructure of explosive joints: Example of titanium to steel cladding. Materials Science & Engineering A: Structural Materials: Properties, Microstructure and Processing, 2011, 528, 2641-2647.	2.6	214
83	Metallic composites processed via extreme deformation: Toward the limits of strength in bulk materials. MRS Bulletin, 2010, 35, 982-991.	1.7	180
84	Design and Characterization of Novel Wear Resistant Multilayer CVD Coatings with Improved Adhesion Between Al ₂ O ₃ and Ti(C,N). Advanced Engineering Materials, 2010, 12, 929-934.	1.6	29
85	Microstructure Characterization of Tool Steel Claddings Coâ€Extruded on Low Alloyed Steel Substrates. Advanced Engineering Materials, 2009, 11, 364-369.	1.6	0
86	Influence of micro-blasting on the microstructure and residual stresses of CVD κ-Al2O3 coatings. Surface and Coatings Technology, 2009, 203, 3708-3717.	2.2	43
87	Microstructure and mechanical properties of magnesium alloy AZ31B laser beam welds. Materials Science & Engineering A: Structural Materials: Properties, Microstructure and Processing, 2008, 485, 20-30.	2.6	98
88	Microstructure and Mechanical Properties of an AA6181â€₹4 Aluminium Alloy to HC340LA High Strength Steel Friction Stir Overlap Weld. Advanced Engineering Materials, 2008, 10, 961-972.	1.6	66
89	EBSD Technique Visualization of Material Flow in Aluminum to Steel Frictionâ€stir Dissimilar Welding. Advanced Engineering Materials, 2008, 10, 1127-1133.	1.6	45
90	Influence of nitridation on surface microstructure and properties of graded cemented carbides with Co and Ni binders. Surface and Coatings Technology, 2008, 202, 5962-5975.	2.2	36

Aleksander Kostka

#	Article	IF	CITATIONS
91	On the contribution of carbides and micrograin boundaries to the creep strength of tempered martensite ferritic steels. Acta Materialia, 2007, 55, 539-550.	3.8	234
92	High-temperature dislocation plasticity in the single-crystal superalloy LEK94. Journal of Microscopy, 2006, 223, 295-297.	0.8	6
93	The software tool for lattice parameters determination from nanoareas using CBED patterns. Materials Chemistry and Physics, 2003, 81, 233-236.	2.0	6
94	TEM study of the interface in ceramic-reinforced aluminum-based composites. Materials Chemistry and Physics, 2003, 81, 323-325.	2.0	20